Combinatorial observation ionospheric characteristics during tropical cyclone Debbie passing eastern Australia in 2017 using GPS and ionosonde

Fuyang Ke[1], Jinling Wang[2], Kehe Wang[3], Jiujing Xu[4], Yong Wang[5], Xinzhi Wang[1], Jian Deng[6]

[1]School of Remote Sensing and Geomatics Engineering, Nanjing University of Information Science & Technology, Nanjing 210044, China

[2]School of Civil and Environmental Engineering, The University of New South Wales, Sydney, 2025, Australia

[3]Space Weather Services, Bureau of Meteorology, Surry Hills, New South Wales, Australia

[4]School of Geodesy and Geomatics, Anhui University of Science and Technology, Huainan 232001, China

[5]Jiangsu Province Surveying and Mapping Engineering Institute, Nanjing 210013, China

[6]School of Computer and Information Engineering, Xiamen University of Technology, Xiamen 361024, China

Correspondence to: Fuyang Ke (ke.fuyang@qq.com)

Abstract. The ionospheric morphology responses to tropical cyclone passing over eastern Australia, named as DEBBIE in 2017, is investigated using Global Positioning System (GPS) Slant Total Electron Content (STEC), GPS ionospheric scintillation S_4 index and ionospheric characteristics by ionosonde. Based on the data analysis in this study, some significant morphological characteristics of ionospheric responses to tropical cyclone Debbie are identified as follows: a) As the GPS satellites PRN01 and PRN11 were passing above typhoon centre, their ROTI (Rate of STEC index) values are obviously increased. b) The S_4 intensity of the GPS ionospheric scintillations is significantly enhanced on March 27, which mostly concentrate around tropical cyclone centre and distribute over the region within 18 °S-25 °S. c) The stronger enhancement of f_0F1 and f_0F2 are observed by ionosonde at Townsville on March 28, when the distance between Townsville and the centre of tropical cyclone Debbie was shorter. Regarding the coupling mechanism between the ionospheric disturbance and the tropical cyclone, it is supposed that the electric field perturbations due to turbulent top movement from tropical cyclones might generate ionospheric irregularity and disturbance. When radio signals encounter the bubbles produced by some ionospheric irregularities, the ionospheric scintillations occur.

1. Introduction

It is acknowledged that the ionosphere is one important and indispensable part of atmosphere for earth and a complex physical system (Wu et al., 1996). The ionospheric irregularity and disturbance can degrade the operation reliability of ground-based radio and GPS. Even it can lead to their failure due to loss of signal lock. Normally, ionospheric disturbances are majorly caused by the strong solar and geomagnetic activity. It has been indicated that ionospheric dynamics behaviours at low, mid and high latitude are dominated by solar tides and horizontal geomagnetic field lines, the inner magnetosphere and neutral winds, and the solar wind and electron precipitation, respectively (Skone et al., 2001). The lower layer of the ionosphere is also connected to the neutral atmosphere. In the 1950s, Beynon et al. (1953) have pointed out that ionospheric disturbance is related to the atmospheric activity in the troposphere. Moreover, the lower-level atmospheric activity not only can cause the ionospheric structure and physical variation, but also can trigger the small and medium scale ionospheric disturbances (Forbes, 1996).

The tropical cyclone is a typical and strong convective atmospheric activity. Bauer (1958) has firstly discovered one phenomenon of ionospheric response to hurricane passage that f_0F2 and the critical frequency of the ionospheric F2 layer observed by ionosonde began to increase as hurricane approaching to ionosonde observation station. Additionally, the total

40　electron content (TEC) and ionospheric scintillation can be achieved by ground GPS station to study the morphological characteristic of ionospheric response to tropical cyclone (Yang and Liu, 2016). Some previous studies have shown that the anomalies of TEC increment were detected during typhoon Matsa in 2005 (Mao et al., 2010), Aili in 2004 (Cheng et al., 2013), Nakri in 2008 (Lin, 2012), Tembin in 2012 (Yang and Liu, 2016) and Typhoon Meranti in 2016 (Chou et al., 2017). However, it is contrarily demonstrated that the TEC around the equatorial area decreases during typhoon Mahasen in 2013

45　and Hudhud in 2014 passing over the Indian sector (Guha et al., 2016). Meanwhile, the previous results have shown that the ionospheric disturbances are emanating outward and lasting for more than 10 h before Super Typhoon Meranti in 2016 landfall (Chou et al., 2017), and that the number of radio occultation scintillation increases to the peak as typhoon Tembin in 2012 closest to Hong Kong (Yang and Liu, 2016). The results of statistical analysis have shown that ionospheric disturbance percentage of 24 strong typhoons in China (Xiao et al., 2007), 41 tropical cyclones in the Atlantic Ocean (Nina et al., 2017),

50　and 25 hurricanes in western and central part of the Czech Republic (Šindelářová et al., 2009) are 92%, 88% and 8%, respectively. Furthermore, the characteristics of ionospheric disturbance intense are not the same. Although the results (Xiao et al., 2007; Rice et al., 2012; Yu et al., 2010; Ke et al., 2018) show that the f_0F2 values increase during the studied tropical cyclones, the studies (Liu et al., 2006; Rozhnoi et al., 2014) demonstrate that they decrease. Using the ionosonde instruments on board the Cosmos 1809 satellite (Isaev et al., 2010), it is indicated that the pressure of the electron gas,

55　electric field and scintillation intense increase in some specific zones. But plasma density and pressure above typhoon eye sharply decrease along with typhoon intensification.

In summary, there are still some uncertainty about morphological characteristics of ionospheric disturbances caused by tropical cyclones (Perevalova et al., 2011; Zakharov & Kunitsyn, 2012). Moreover, the ionospheric response to tropical cyclones in the southern hemisphere are rarely studied. Therefore, the previous studies are still limited not only in

60　ionospheric observation instrument but also in the representative of the tropical cyclone cases studied worldwide. In the southern hemisphere, there are several ionosonde and GPS continuously operating reference stations (CORS) distributed around Australia for detecting the ionospheric morphological parameters. In March 2017, tropical cyclone Debbie is the strongest tropical cyclone in the Australian region since tropical cyclone Quang in 2015, which is branded the most dangerous cyclone to impact Queensland since tropical cyclone Yasi in 2011. The combination observation of ionosonde,

65　GPS STEC and GPS ionospheric scintillation will be utilized to study the morphological characteristics of ionospheric response to tropical cyclone Debbie as a representative case in the southern hemisphere.

Additionally, there are also some controversies about the coupling mechanism between tropical cyclones and ionospheric disturbance. Hung et al. (1978) of NASA in the United States have found the existence of gravity waves and mesoscale disturbances in the F layer of the ionosphere during the tornado eruption using ionosonde, and considered that the gravity

70　wave may be the main source of ionospheric disturbance. It is suggested (Shen, 1982; Liu, et al. 2006; Wang, et al. 2005) that the turbopause motion is a possible mechanism for the interaction between the lower layers of the atmosphere and ionosphere. It is considered that the electric field disturbance in typhoon or hurricane is activated by the ionospheric disturbance caused by the current perturbation from the charged water droplets and aerosols transmitted upward (Isaev 2002, 2010). So, the study on tropical cyclone Debbie is also valuable to realize the coupling mechanism between ionospheric

75　disturbances and tropical cyclones.

In the following section, the using dataset and methodology are firstly introduced. Then, the ionospheric response to tropical cyclone Debbie in 2017 will be analysed for demonstrating the morphological characteristics of ionospheric response to tropical cyclone Debbie in the southern hemisphere. Meanwhile, the possible coupling mechanism of reaction between ionospheric disturbance and tropical cyclone will be discussed.

2. Dataset

2.1 Tropical cyclone Debbie and ionospheric dataset
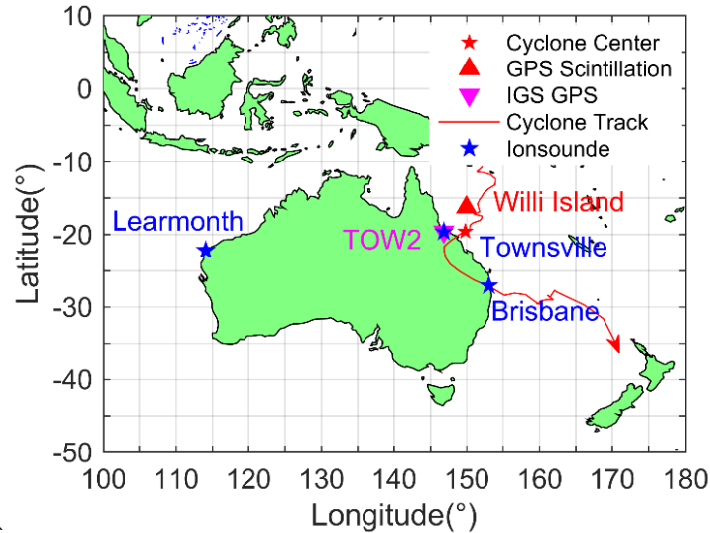
Figure 1：GPS station of Ionospheric Scintillation Monitors (Red triangle: Willi Island), International GNSS Station (Pink triangle: TOW2), Ionosonde Stations (Blue triangles: Learmonth, Townsville, Brisbane), the path of tropical cyclone DEBBIE
85 **(Red line), the tropical cyclone moving directions (arrow) and the place with the largest wind velocity (Red pentagram)**

Tropical cyclone Debbie is formed above the south of Solomon Sea of South Pacific at Universal Time (UT) 12:00 of 21 Mar 2017. Then it lands on Hook Island of Queensland at UT00:00 on 28 Mar 2017 at the speed of 105 knots（about 54 m/s）. Tropical cyclone Debbie left the Australian continent from Brisbane at 12:00 on 30 Mar 2017. As shown in Figure 1, tropical cyclone Debbie moves from north to south and its impact zone is in medium geomagnetic latitude from $15°$S to

90 $60°$S in the southern hemisphere. Tropical cyclone Debbie centre passes above Willi GPS ionospheric scintillation station, Townsville and Brisbane Ionosonde stations, TOW2 GPS stations. When tropical cyclone Debbie lands on Hook Island of Queensland, the ellipsoidal distances between the tropical cyclone centre and the observation stations of Willis, Townsville and Brisbane are 460 km, 230 km and 925 km, respectively.

2.2 Solar and geomagnetic field activity
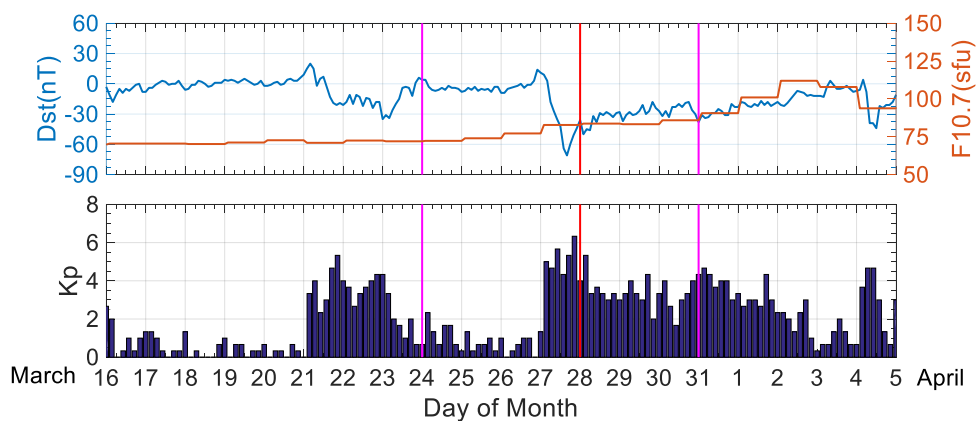
95

Figure 2：The solar index F10.7, the Dst and Kp indexes of geomagnetic field from16 March to 5 April 2017

The ionospheric activity is mainly dominated and affected by the solar and geomagnetic activities. Hence, the influence from the solar and geomagnetic field should be firstly analysed before studying the ionospheric response to tropical cyclone. Normally, the solar radio flux (10.7cm/2800MHz, F10.7), Dst and Kp geomagnetic activity indexes are used to judge the

100 solar and geomagnetic activity level, respectively. Their variations during tropical cyclone Debbie are shown in Figure 2.

3

Generally, the F10.7 ranges of [70sfu, 100sfu], [100sfu, 150sfu], and [150sfu, 250sfu] represent low, moderate, and high level of solar activity, respectively [Wang et al., 2015]. The Dst ranges of $-50\,\text{nT} < \text{Dst} \le -30\,\text{nT}$, $-100\,\text{nT} < \text{Dst} \le -50\,\text{nT}$, $-200\,\text{nT} < \text{Dst} \le -100\,\text{nT}$ and $\text{Dst} \le -200\,\text{nT}$ signify small, moderate, large and stronger and severe geomagnetic storms, respectively [Mao et al., 2010]. The Kp index ranges of 0-1, 2-4, 5, 6, and 7-9 denote quiet geomagnetic field, unstable geomagnetic field, small geomagnetic storm, large geomagnetic storm and severe geomagnetic storm, respectively. It is shown that the solar activity during tropical cyclone Debbie is at low level with F10.7 less than 100 sfu. But the Dst and Kp indexes indicate there are some a small geomagnetic storm on 27 March 2017 before cyclone Debbie landed on Hook Island of Queensland at UT00:00 on 28 Mar 2017. Therefore, the influence on ionosphere from the small geomagnetic storm should not be ignored to study the ionospheric response to tropical cyclone Debbie.

3 Methodology

2.1 The Rate of GPS STEC

The rate of GPS slant TEC (ROT) is as a measurement of GPS phase fluctuation, which can be used to monitor the ionospheric irregularity and disturbance. It represents the derivative of GPS slant TEC between two successive epochs, which can be calculated by the following equation (Yang and Liu, 2016):

$$\text{ROT} = \frac{\text{STEC}_k^i - \text{STEC}_{k-1}^i}{t_k - t_{k-1}} \tag{1}$$

where i is the number of a GPS satellite; t_k is an epoch time; the unit of ROT is TECU/min.

Rate of STEC index (ROTI) indicates the extent of the GPS phase fluctuations, which can be used to detect the occurrence of the ionospheric irregularities by the sharp TEC gradient. The ROTI represents the standard deviation of the ROT in a specific time interval (Yang and Liu, 2016):

$$\text{ROTI} = \sqrt{\langle \text{ROT}^2 \rangle - \langle \text{ROT} \rangle^2} \tag{2}$$

where the angle brackets denote the average value in a 5-min observation time interval.

2.2 GPS ionospheric Scintillation

The intense of GPS ionospheric scintillation is typically quantified by the S_4 index, which is calculated using the following equation (Kintner et al., 2007):

$$S_4 = \sqrt{\frac{\langle I^2 \rangle - \langle I \rangle^2}{\langle I \rangle^2}} - \sqrt{\frac{100}{\overline{\frac{C}{N_0}}}\left[1 + \frac{500}{19\overline{\frac{C}{N_0}}}\right]} \tag{3}$$

where I is the intense of GPS signal, which is output from the GPS receiver tracking loop. $\overline{C/N_0}$ is the average Signal-to-Noise Ratio of satellite L1 Band in an observation period. If S_4 is more than 0.2, it indicates strong GPS ionospheric scintillation (Muella et al., 2008).

2.3 Ionospheric characteristics by Ionosonde

The ionospheric parameters of f_0E, f_0F1, and f_0F2 can be used to analyse the ionospheric response to cyclone in vertical direction. Accordingly, the electron density N_e in each layer can be calculated using the frequency of reflection radio wave by the follow equation:

$$N_e = 1.24 \times 10^{10} f^2 \tag{4}$$

where f is the critical frequency f_0E, f_0F1 and f_0F2 for the corresponding plasma with electron density N_e. The units of f and N_e are MHz and m^{-3}, respectively. The electron density N_e is positively linear dependent on f^2. Hence, the parameters of f_0E, f_0F1, f_0F2 can reflect the electron density variation of ionosphere in vertical layers in response to tropical cyclone.

4. Analysis Result and Discussion

### 4.1 GPS STEC response to tropical cyclone Debbie
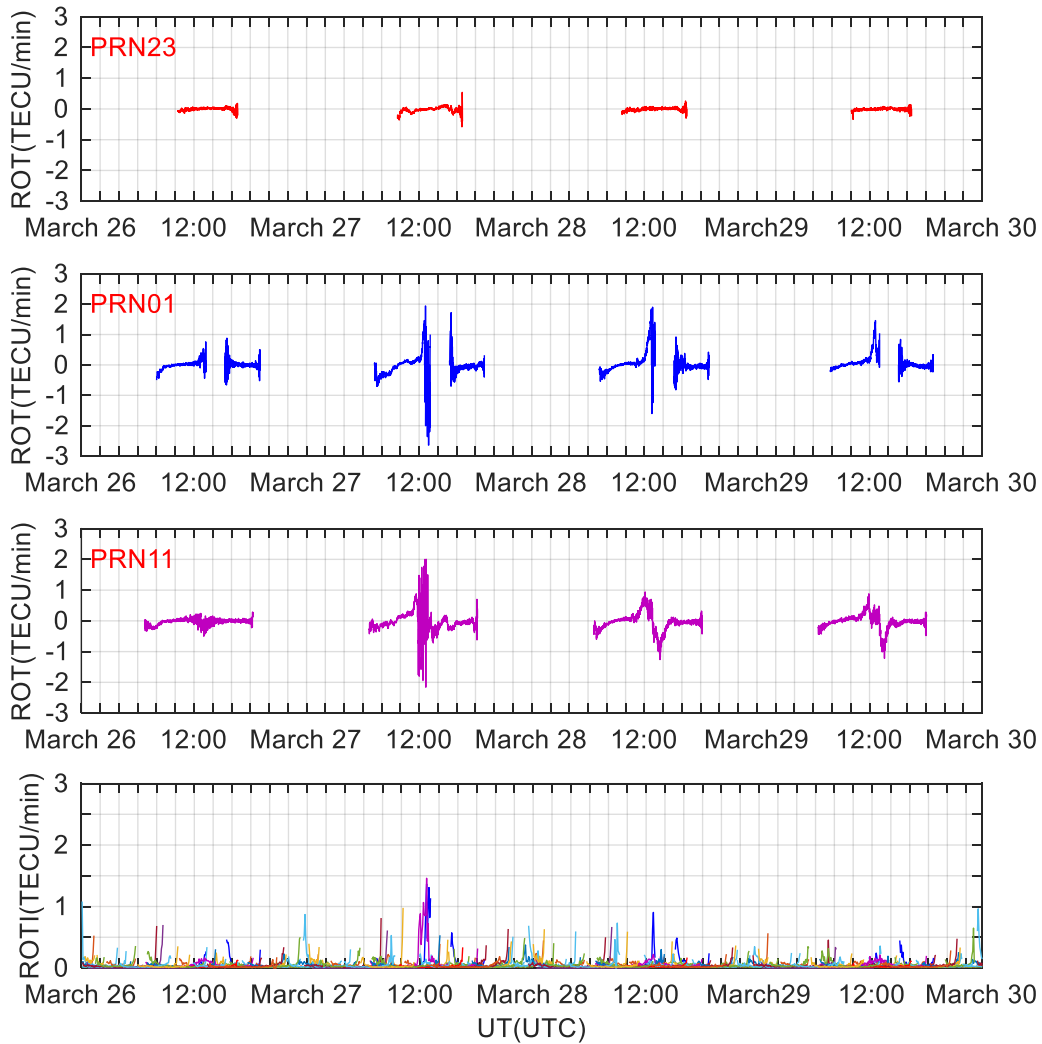
Figure 3: The variation of ROT for GPS PRN23, PRN01 and PRN11 and ROTI (5min) of all GPS satellites during March 26-29 over the TOW2 IGS station.

The GPS STEC response to tropical cyclone Debbie passing from 26-29 March 2017 is firstly analysed. The GPS STEC is extracted from TOW2 IGS station, which tropical cyclone Debbie passes above. The variation of ROT for PRN23, PRN01 and PRN11 and ROTI (5min) for all satellites during March 26-29 are shown in Figure 3. It shows that ROTI has an evident increment on UT 12:00 (Local Time (LT) =UT+8h) March 27, the day before tropical cyclone Debbie centre landed on Hook Island. When tropical cyclone Debbie centre landed on Hook Island of Queensland on March 28, the increment of ROTI is smaller. As shown in the top three of Figure 3, the variation of ROT for PRN01 and PRN11 are obviously increased as tropical cyclone Debbie landing. The Ionospheric Pierce Point (IPP) traces of GPS PRN01 and PRN11 satellites over TOW2 station are above the impact area of tropical cyclone Debbie on 28 March. The variation of ROT for PRN23 is not obvious, because the IPP trace of GPS PRN23 over TOW2 station is far away from the cyclone. Despite there is a small

geomagnetic storm on 27 March, GPS STEC extracted by the other GPS satellites far away from tropical cyclone Debbie are

155   not anomalous. Therefore, it can be inferred that the anomaly of ROTI and ROT extracted by GPS PRN01 and PRN11 above

tropical cyclone centre on UT12:00 of 27 and 28 March are more likely triggered by cyclone Debbie.

4.2 GPS ionospheric scintillation response
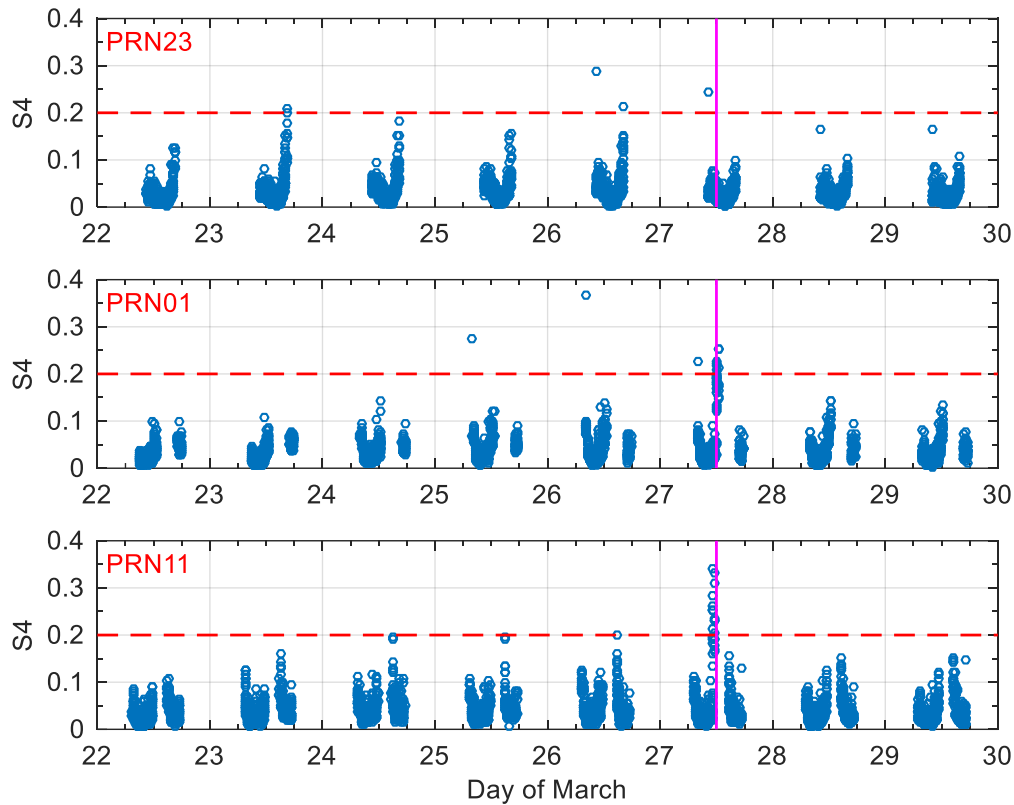
Figure 4: The GPS ionospheric scintillation S4 variations of GPS PRN23, PRN01 and PRN11 satellites during 22-29 March 2017.
160   **The dotted red line is the threshold of the strong GPS ionospheric scintillation. The magenta vertical line denotes the time point when cyclone Debbie centre was the closest to GPS station**

Although ionospheric scintillation can degrade the GPS signal quality or even cause failure of the signal lock, GPS also

provides a new tool for detecting ionospheric irregularity and scintillation. GPS scintillation amplitude index S_4 more than

0.2 indicates strong ionospheric scintillation. Figure 4 shows that the variation of GPS ionospheric scintillation of PRN23,

165   PRN01 and PRN11 above Willi Island GPS station during the period of 22-29 March 2017. It shows that the geomagnetic

field is with a small storm in Figure 2. Theoretically, the affection on ionospheric scintillation of GPS PRN01 and PRN11

should be approximately same under the same geomagnetic storm. When the distance from tropical cyclone centre to Willis

station is 370 km along with the wind speed of 54 m/s at midnight of 27 March, the number and intensity of S4>0.2 observed

by GPS satellite PRN01 and PRN11 near to the tropical cyclone centre are more and larger than those at the other time in

170   Figure 4. But the S4 observed by GPS satellite PRN23 far away from the tropical cyclone centre are not obviously abnormal

in Figure 4. Hence, it can be deduced that the number increment and enhance of GPS ionospheric scintillations might be

triggered by tropical cyclone Debbie on March 27.
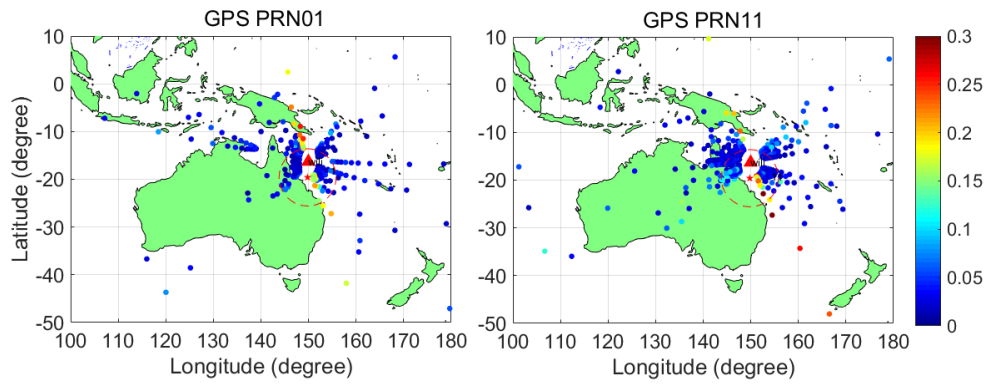
Figure 5：Ionospheric pierce point traces and GPS ionospheric scintillation S_4 intensity of GPS PRN01 and PRN11 satellites through cyclone Debbie on March 27. The red dashed cycles indicate the area affected by cyclone Debbie. The colourful solid circles are GPS ionospheric scintillations and their intensity

To further determine the correlation between GPS ionospheric scintillation and tropical cyclone Debbie, the spatial relations between GPS ionospheric scintillation points `pierce` into ionosphere and tropical cyclone Debbie are shown in Figure 5. It is obvious that more points of S_4>0.2 are mainly distributed around the tropical cyclone centre. What is more that the intensity and number of the points of S_4>0.2 above the area of $18°S - 25°S$ in the latitude and $150°E - 155°E$ in the longitude around tropical cyclone center ($B = 19.6°S, L = 149.8°E$) is stronger and larger than those above the other area. Normally, the occurrence of strong ionospheric scintillations is more frequent in low geomagnetic latitude ($\pm15°$) and high geomagnetic latitude ($\pm70°$). Nevertheless, the area of these GPS ionospheric scintillations with S_4>0.2 doesn't belong to the area of frequent ionospheric scintillation. The evidence further verified that the strong ionospheric scintillations might be triggered by tropical cyclone Debbie.

### 4.3 The ionospheric parameters in E/F1/F2 layer by Ionosonde

The ionosphere is divided into D, E, F1 and F2 layers. There are differences in the characteristics of the ionosphere in each layer. However, it is difficult to distinguish the characteristics of the ionosphere in each layer in response to tropical cyclone Debbie only used by GPS. Therefore, Ionosondes installed in Townsville and Brisbane are used to detect and analyse the characteristic parameters of f_0E, f_0F1 and f_0F2 in E, F1 and F2 layer for ionospheric response to cyclone Debbie. With regard to characteristic parameters f_0E, f_0F1 and f_0F2, the monthly median values from 24 to 31 March are referred as their normal values compared with the electron density response to tropical cyclone in vertical layers.
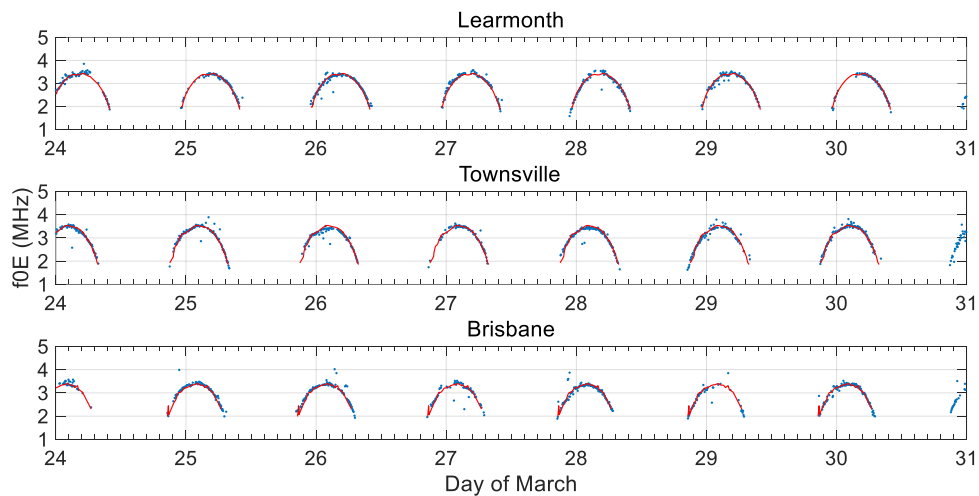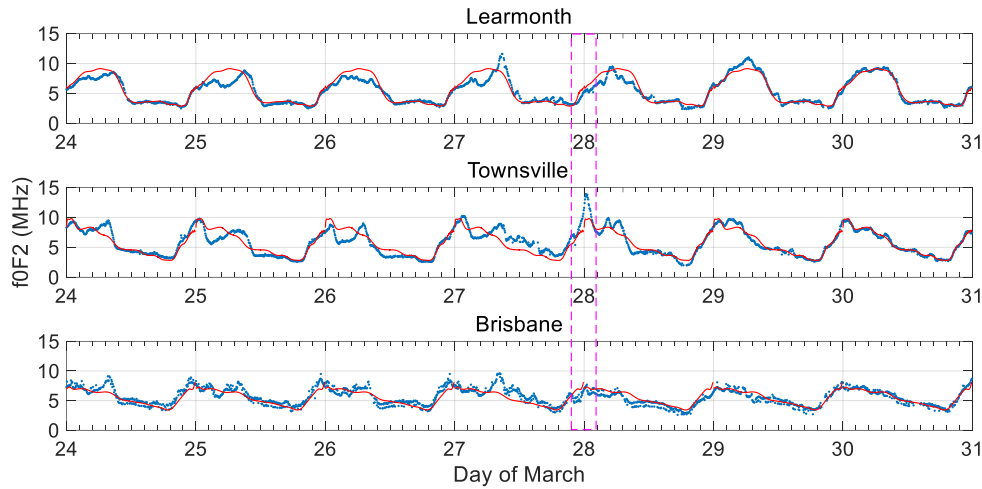

Figure 6：The f_0E variation in the ionospheric E layer at Learmonth, Townsville and Brisbane Ionosonde stations from 24 to 30 March in 2017 as tropical cyclone Debbie moving. The f_0E is the ordinary wave critical frequency of the lowest thick layer which causes a discontinuity. The red lines denote the monthly median value of f_0E from 24 to 30 March

The characteristic parameters f_0E in the ionospheric E layer observed by Townsville and Brisbane Ionosonde stations as tropical cyclone Debbie moving from 24 to 30 March are shown in Figure 6. In spite of f_0E values observed by Townsville Ionosonde are small enhanced and elevated at midday of 29 and 30 March after tropical cyclone Debbie landfall, the f_0E values observed by Learmonth, Townsville and Brisbane Ionosondes on landfall day and other days are not significantly anomalous compared their monthly median values. The f_0E observed by Learmonth, Townsville and Brisbane Ionosondes are all approximately equal. The ranges of f_0E and virtual height (h'E) are from 1.7 to 4.0 MHz and from 85 km to 100 km, respectively. The phenomenon in the ionospheric E layer indicates that tropical cyclone Debbie could not disturb the ionosphere in E layer.
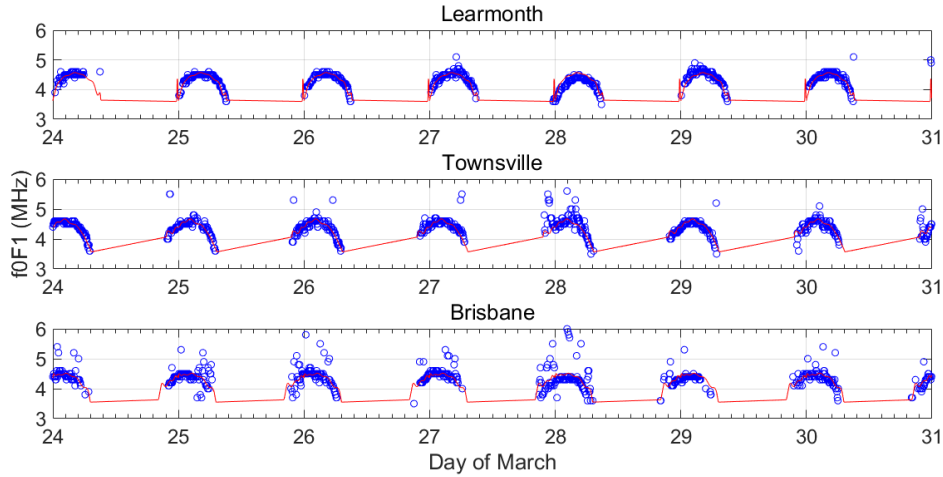
Figure 7：The f_0F1 variation in the ionospheric F1 layer at Learmonth, Townsville and Brisbane Ionosonde stations from 24 to 30 March in 2017 as tropical cyclone Debbie moving. The f_0F1 is the ordinary wave F1 critical frequency. The red lines denote the monthly median value of f_0F1 from 24 to 30 March

Figure 8：The f_0F2 variation in the ionospheric F2 layer at Learmonth, Townsville and Brisbane Ionosonde stations from 24 to 30 March in 2017 as tropical cyclone Debbie moving. The f_0F2 is ordinary wave critical frequency of the highest stratification in the F region. The red lines denote the monthly median value of f_0F2 values from 24 to 30 March. The pink rectangular is tropical cyclone Debbie landfall day

The ionospheric parameters f_0F1 and f_0F2 on Learmonth, Townsville and Brisbane Ionosonde stations as tropical cyclone Debbie moving from 24 to 30 March are shown in Figure 7 and Figure 8. It is obvious that the f_0F1 and f_0F2 intensity on Townsville station on 28 March are significantly stronger than the monthly median value. Meanwhile, the f_0F2 intensity on Learmonth and Brisbane far away from tropical cyclone Debbie centre are approximately equal to the monthly median values under the same solar and geomagnetic activity. Theoretically, the influences on f_0F1 and f_0F2 of Learmonth and Townsville in the same latitude under the same small geomagnetic storm condition on 27 and 28 March should be almost the same. Nevertheless, the anomaly extent of f_0F1 and f_0F2 on Townsville station are significantly larger than those on Learmonth on 28 March. The largest f_0F1 deviation relative to the monthly median value on Townsville station is 1.0MHz -

8

1.5MHz. Additionally, the largest f_0F2 deviation relative to the monthly median value on Townsville station is 5.0MHz. The electron density N_e is positively related to f_0F1 and f_0F2. Thus, it can be inferred that the electron density of ionospheric F2 layer significantly increased as tropical cyclone Debbie is above Townsville station. Despite the $f0F1$ in F1 layer observed by Brisbane station is also increased on 28 March in Figure 7, the periodic anomaly of $f0F1$ in those day might be due to Ionosonde noise. Therefore, the stronger enhancement of f_0F1 and f_0F2 observed by Townsville Ionosonde station on 28 March should be attributed to tropical cyclone Debbie.

4.3 The mechanism of ionospheric response to tropical cyclone
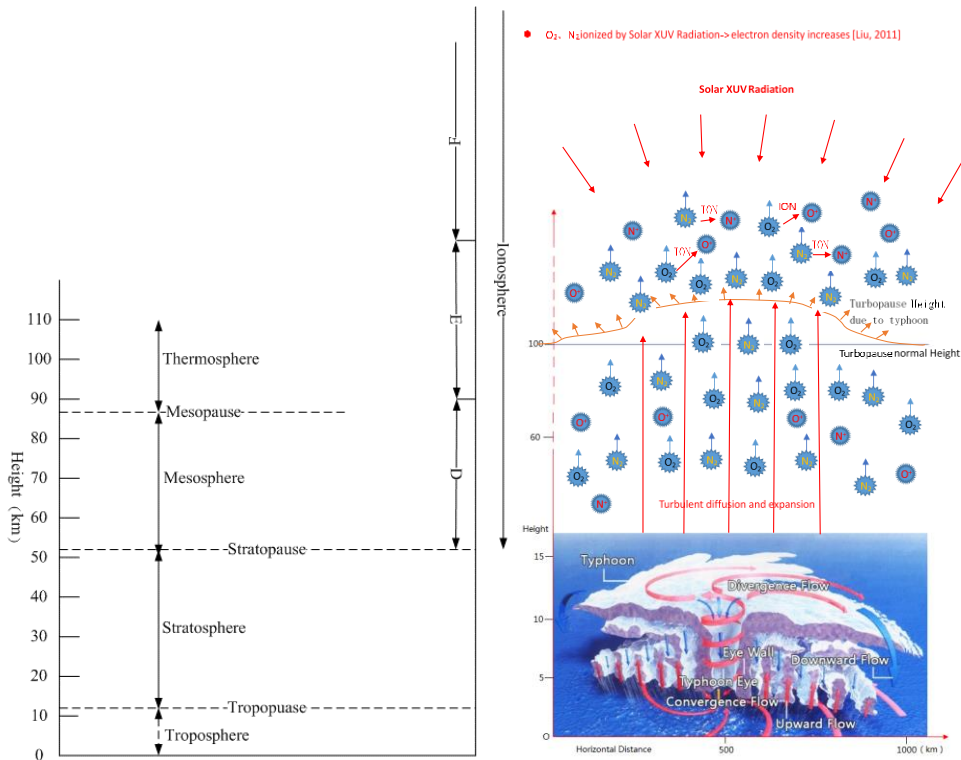
Figure 9: Profile of atmosphere and tropical cyclone structure (From China Meteorological Administration http://www.cma.gov.cn) and the schematic diagram of ionospheric response to tropical cyclone

The results reveal that the ionospheric irregularity and disturbance could be likely related to tropical cyclone Debbie. Even it can further produce GPS ionospheric scintillations. However, the coupling mechanism between tropical cyclone and ionospheric disturbances is still indefinite and controversial. The previous studies considered that the source of ionospheric disturbance might be from gravity waves generated by tropical cyclone (Xiao, et al. 2007), an atmosphere divergence/convergence model and dynamic coupling (Shen, 1982), a disturbed electric field caused by tropical cyclone (Isaev, et al. 2002), turbulent top layer movement of tropical cyclone (Shen, 1982; Liu, et al. 2006; Wang, et al. 2005) and lighting discharge from clouds of tropical cyclone (Shao, et al. 2013). Nevertheless, the vertical gravity waves could not disturb the more than 100 km height ionosphere in effective range due to its dozens of kilometres wavelength. Especially, it is much difficult to explain why f_0F2 in more than 300 km height F2 ionospheric layer observed by Townsville Ionosonde station is larger than the monthly median value as tropical cyclone Debbie was landing on 28 March in Figure 8. Assuming that gravity waves can cause ionospheric disturbances, the $f0E$ in ionospheric E layer should be also anomalous. On the contrary, the $f0E$ is approximately equal to the monthly median value in Figure 6. It is also difficult to explain the phenomenon only using the turbulent top layer movement of tropical cyclone and the disturbed electric field above the tropical cyclone. Because the tropical cyclone belongs to airflow system in troposphere with a height of 20 km or less and

might not directly affect the ionosphere with a height of 50 km or more in the left of Figure 9. Furthermore, the short-term lightning could not explain the long-term ionospheric disturbances for about 2 hours in Figure 8.

Therefore, it is supposed that the ionospheric disturbance in response to tropical cyclone Debbie is interacted by multi-source
250 of turbulent top layer movement, electric field and electron photochemical reactions. The strong tropical cyclone airflows can lead to the structure change of stratosphere and mesosphere. Among them, the upward airflow will continue to develop upward due to the temperature structure of the middle layer and elevate the turbulence layer with about 100km height (Shen, 1982). By contrary, the airflow direction of the tropopause above tropical cyclone centre is downward. According to atmospheric turbulence layer movement theory (Liu, et al. 2006), the airflows from the tropical cyclone will make the
255 turbulent diffusion coefficient increase and the molecular diffusion coefficient decrease. As a result, some neutral molecules (N_2, O_2) in E layer will be taken into the ionospheric F1 and F2 layer. X-rays and extreme ultraviolet rays from the sun can make these neutral molecules to ionize and produce free electrons and ions leading to the increment of electron density in F1 and F2 layer (Liu, et al. 2011). Therefore, it can be explained the phenomenon that the f_0F1 and f_0F2 on Townsville station are significantly enhanced as tropical cyclone Debbie is above Townsville station in Figure 7 and Figure 8. Along with the
260 increment of electrons, the balance of electric field is destroyed. The growth of Rayleigh–Taylor instability from the electric field perturbations can lead to some ionospheric irregularities in the F layer (Prakash 1999), which may have velocity shear mixing within the hole gradients (Kelley 1985). When the hole arrives at the topside of F layer, the bubble is produced. As it happens that GPS signal encounters the bubble, ionospheric scintillation will occur. Therefore, it can explain why there are just some ionospheric scintillations of PRN01 and PRN11 above tropical cyclone Debbie, whose values of S_4 are more than
265 0.2 in Figure 5. Moreover, the S4 of ionospheric scintillations of PRN01 and PRN11 observed by Townsville station is more than 0.2 on the midday of 27 March 2017 in Figure 4. Meanwhile, the f_0F2 in ionospheric F2 layer is enlarged at the same time in Figure 8. Thus it can be supposed that the ionospheric scintillation is produced by the ionospheric irregularities in F2 layer due to tropical cyclone Debbie.

5. Conclusions

270 The morphological characteristics of ionospheric response to tropical cyclone Debbie passing eastern Australia in 2017 is investigated by GPS and ionosonde. The results agree with the previous viewpoint that tropical cyclone can trigger ionospheric disturbance. The morphological characteristics of ionospheric response to tropical cyclone Debbie can be summarized as follows.

(1) As the GPS satellites PRN01 and PRN11 were passing over tropical cyclone Debbie, their ROTI and ROT are
275 significantly increased. (2) The S_4 intensity of GPS ionospheric scintillations is enhanced on March 27, which mostly concentrate above tropical cyclone centre and distribute over the region of $18^\circ S - 25^\circ S$ in the latitude and $150^\circ E - 155^\circ E$ in the longitude around tropical cyclone centre (B $= 19.6^\circ S, L = 149.8^\circ E$)。 (3) Compared with those on Learmonth and Brisbane, the intensity of f_0F1 and f_0F2 on Townsville was obviously increased as tropical cyclone Debbie landed on 28 March. At the same time, distance between Townsville and the tropical cyclone centre is the shortest.

280 Considering the influence from the geomagnetic and solar activity, the turbulent top movement theory is utilized to explain how tropical cyclone causes ionospheric irregularity and further triggers ionospheric scintillations. It is assumed that the turbulent top movement of tropical cyclone can break the balance of the electric field. Then, the electric field perturbations can contribute to the growth of Rayleigh-Taylor instability producing ionospheric disturbance in the F layer of the ionosphere. Furthermore, the ionospheric density irregularities can form drift waves to create bubbles in F layer. When GPS
285 signals encounter the bubbles, GPS ionospheric scintillations can appear.

References

295 Bauer S. J.: An apparent ionospheric response to the passage of hurricanes, Journal of Geophysical Research, 63: 265-269, 1958.

Beynon W. J. G., and Brown G. M.: Geophysical and meteorological changes in the period January-April 1949, Nature, 167: 1012-1014, 1953.

Cheng G. Sh., Cheng Y., and Du Y. J.: Research on disturbance of No.0418 typhoon "AiLi" to TEC, Journal of natural 300 disasters, 22: 84-90, 2013.

Chou M. Y., Lin C. C. H., Yue J., Tsai H. F., Sun Y. Y., Liu J. Y., and Chen C. H.: Concentric traveling ionosphere disturbances triggered by Super Typhoon Meranti (2016), Geophysical Research Letters, 44: 1219-1226, 2017.

Forbes J. M.: Planetary waves in the thermosphere-ionosphere system, Earth Planets and Space, 48: 91-98, 1996.

Guha A., Paul B., Chakraborty M., and De B. K.: Tropical cyclone effects on the equatorial ionosphere: First result from the 305 Indian sector, Journal of Geophysical Research Space Physics, 121: 5764–5777, 2016.

Isaev N. V., Kostin V. M., Belyaev G. G., Ovcharenko O. Y., and Trushkina E. P.: Disturbances of the Topside Ionosphere Caused by Typhoons, Geomagnetism and Aeronomy, 50 (2): 253–264, 2010.

Isaev, N. V., Sorokin, V. M., and Chmyrev, V. M.: Ionospheric electric fields related to sea storms and typhoons, Geomagnetism & Aeronomy, 42: 638-643, 2002.

310 Ke F., Wang J., Tu M., Wang X., Wang X., Zhao X., Deng J.: Morphological characteristics and coupling mechanism of the ionospheric disturbance caused by Super Typhoon Sarika in 2016, Advances in Space Research, 62(5), 1137-1145, 2018.

Kelley M.C.: Equatorial spread F: Recent results and outstanding problems, Journal of atmospheric and terrestrial physics, 47: 745-752, 1985.

Kintner P. M., Ledvina B. M., and Paula E. R.: GPS and ionospheric scintillation, Space Weather, 5: S09003, 2007.

315 Lin J. W.: Ionospheric total electron content anomalies due to Typhoon Nakri on 29 May 2008：A nonlinear principal component analysis, Computers & Geosciences, 46: 189-195, 2012.

Liu L. B., Wan W. X., Chen Y. D., et al.: Solar activity effects of the ionosphere: A brief review, Chinese Science Bulletin, 56, 2011.

Liu, Y. M., Wang, J. S, Xiao, Z., and Suo, Y. Ch.: A possible mechanism of typhoon effects on the ionospheric F2 layer, 320 Chinese Journal of Space Science, 26: 92-97, 2006.

Mao T., Wang J. S., Yang G. L., Yu T., Ping J. S., and Suo Y. C.:. Effects of typhoon Matsa on ionospheric TEC, Chinese Science Bulletin, 55(8): 712-717. (In Chinese), 2010.

Muella M, E de Paula, I Kantor, I Batista, J Sobral, M Abdu, P Kintner, K Groves, P Smorigo: GPS L-band scintillations and ionospheric irregularity zonal drifts inferred at equatorial and low-latitude regions, Journal of Atmospheric and Solar-Terrestrial Physics, 70 (10):1261–1272, 2008.

Nina A., Radovanovic´M., Milovanovic´B., Kovacˇevic´A., Bajcˇetic´J., and Popovic´L.: Low ionospheric reactions on tropical depressions prior hurricanes, Advances in Space Research, 60: 1866–187, 2017.

Perevalova N. P., Ishin A. B.: Effects of Tropical Cyclones in the Ionosphere from Data of Sounding by GPS Signals, Izv Atmos Ocean Phy, 47 (9):1072–1083, 2011.

Prakash S.: Production of electric field perturbations by gravity wave winds in the E region suitable for initiating equatorial spread F, J Geophys Res, 104:10051-10069, 1999.

Rice D. D., Sojka J. J., Eccles J. V., and Schunk R. W.: Typhoon Melor and ionospheric weather in the Asian sector: A case study, Radio Science, 47: RS0L05, 2012.

Rozhnoi A., Solovieva M., Levin B., Hayakawa M., and Fedun V.: Meteorological effects in the lower ionosphere as based on VLF/LF signal observations, Natural Hazards and Earth System Sciences, 14: 2671–2679, 2014.

Shen C.: The correlations between the typhoon and the f0F2 of ionosphere, Chin J Space Sci, 2(4):335-340. (In Chinese), 1982.

Šindelářová T., Burešová D., Chum J.: Observations of acoustic-gravity waves in the ionosphere generated by severe tropospheric weather, Studia Geophysica et Geodaetica, 53(3): 403-418, 2009.

Skone S., Knudsen K., and Jong M.de. Limitations in GPS receiver tracking performance under ionospheric scintillation conditions, Physics and Chemistry of the Earth, 26(6-8): 613-621, 2001.

Wang H. B., Xiong J. N., and Zhao C. Y.: The Mid-term Forecast Method of Solar Radiation Index, Chinese Astronomy and Astrophysics, 39: 198-211, 2015.

Wu, J., Quan, K. H., Dai, K. L., et al.: Progress in the study of the Chinese reference ionosphere, Advances in Space Research, 18(6), 187-190, 1996.

Xiao, Z., Xiao, S. G., Hao, Y. Q., and Zhang D. H.: Morphological features of ionospheric response to typhoon, Journal of Geophysical Research, 112, A04304: 213-220, 2007.

Yang Z., and Liu, Z.: Correlation between ROTI and Ionospheric Scintillation Indices using Hong Kong low-latitude GPS data, GPS Solutions, 20: 815-824, 2016.

Yu T., Wang Y. G., Mao T., Wang J. S., Wang S. Y., Shuai F. H., Su W. D., and Li J. T.: A case study of the variation of ionospheric parameter during typhoons at Xiamen, Acta Meteorologica Sinica, 68: 569-576. (in Chinese), 2010.

Zakharov V. I., Kunitsyn V. E.: Regional Features of Atmospheric Manifestations of Tropical Cyclones according to Ground Based GPS Network Data, Geomagn Aeronomy, 52 (4): 533–545, 2012.